Protein Film Voltammetry of Arsenite Oxidase from the Chemolithoautotrophic Arsenite-Oxidizing Bacterium NT-26†

Paul V. Bernhardt*,‡ and Joanne M. Santini§

Centre for Metals in Biology, Department of Chemistry, University of Queensland, Brisbane, 4072 Queensland, Australia, and Department of Microbiology, La Trobe University, 3086 Victoria, Australia

Received November 2, 2005; Revised Manuscript Received January 19, 2006

ABSTRACT: The chemolithoautotrophic bacterium NT-26 (isolated from a gold mine in the Northern Territory of Australia) is unusual in that it acquires energy by oxidizing arsenite to arsenate while most other arsenic-oxidizing organisms perform this reaction as part of a detoxification mechanism against the potentially harmful arsenite [present as $As(OH)_3$ at neutral pH]. The enzyme that performs this reaction in NT-26 is the molybdoenzyme arsenite oxidase, and it has been previously isolated and characterized. Here we report the direct (unmediated) electrochemistry of NT-26 arsenite oxidase confined to the surface of a pyrolytic graphite working electrode. We have been able to demonstrate that the enzyme functions natively while adsorbed on the electrode where it displays stable and reproducible catalytic electrochemistry in the presence of arsenite. We report a pH dependence of the catalytic electrochemical potential of −33 mV/pH unit that is indicative of proton-coupled electron transfer. We also have performed catalytic voltammetry at a number of temperatures between 5 and 25 °C, and the catalytic current (proportional to the turnover number) follows simple Arrhenius behavior.

Arsenic (As)[1] contamination is a major environmental concern as the element is extremely toxic to most forms of life (*1*−*5*). Accidental occupational exposure to arsenic is problematic in a number of workplaces such as the mining, pesticide, pharmaceutical, glass, and microelectronics industries. It is now established (*6*) that chronic exposure to high levels of inorganic As may lead to a variety of cancers (skin, bladder, lung, and possibly other organs) in addition to serious skin ailments to name but a few. The metabolic pathways for As in humans are complex but include the formation of organoarsenics which may themselves be active toxic forms (*1*).

The most bioavailable (water soluble) forms of As are when it is present in its trivalent (arsenite) and pentavalent (arsenate) forms. At neutral pH, arsenite is present exclusively as the very weak acid $As(OH)_3$ ($pK_{a1} = 9.2$) while arsenate is usually a mixture of $As(OH)_2O_2^-$ and $As(OH)O_3^{2-}$ ($pK_{a2} = 6.9$). Trivalent As is generally considered to be more toxic to animal and plant life, and there is evidence to suggest that it reacts with thiol groups in proteins; on the other hand, the less toxic pentavalent arsenate is believed to act as a phosphate analogue (*2*).

Despite the known harmful effects of As, there are in fact organisms that require As to survive. One of these is the recently characterized bacterium *Rhizobium* sp. str. NT-26, which was isolated from a gold mine in the Northern Territory of Australia (*7*). This organism grows chemolithoautotrophically with arsenite as the electron donor, dioxygen as the electron acceptor, and HCO_3^-/CO_2 as the sole carbon source and has been found growing on samples of the mineral arsenopyrite (FeAsS, the most common As-containing mineral in the world). The enzyme responsible for the oxidation of arsenite to arsenate in this organism has been isolated and characterized (*8*). It is the molybdenum-containing enzyme arsenite oxidase, which is located in the periplasmic space of the cell. Unlike most other organisms which typically oxidize arsenite for the purpose of detoxification, NT-26 gains free energy from arsenite oxidation.

All known arsenite oxidase enzymes characterized thus far comprise three distinct electron transfer centers: a Mo active site and an adjacent high-potential [3Fe-4S] cluster (within the α subunit) and a Rieske-type [2Fe-2S] center in the β subunit (*9*). The only crystallographically characterized arsenite oxidase is that isolated from the soil bacterium *Alcaligenes faecalis*, and the configuration of the three centers is shown in Figure 1. The Mo active site bears two molybdopterin guanine dinucleotide (MGD) ligands which each chelate the metal ion via a pair of dithiolene S donors. This feature places arsenite oxidase in the DMSO reductase family of molybdoenzymes (*10*). However, arsenite oxidase is unusual in that no ligands are provided by the protein, such as serine, cysteine, aspartate, or selenocysteine seen in other members of the DMSO reductase family. The five-coordinate geometry of the Mo ion in arsenite oxidase is

† P.V.B. acknowledges financial support from an Australian Research Council Discovery Grant (DP0343405). J.M.S. acknowledges support from an Australian Research Council Discovery Grant (DP0209802) and was a recipient of an ARC Australian Postdoctoral Fellowship.

* To whom correspondence should be addressed. Telephone: +61 7 3365 4266. Fax: +61 7 3365 4299. E-mail: P.Bernhardt@uq.edu.au.

‡ University of Queensland.

§ La Trobe University.

[1] Abbreviations: As, arsenic; DMSO, dimethyl sulfoxide; MES, *N*-morpholinoethanesulfonic acid; NHE, normal hydrogen electrode; DDAB, didodecyldimethylammonium bromide.

10.1021/bi0522448 CCC: $33.50
Published on Web 02/10/2006

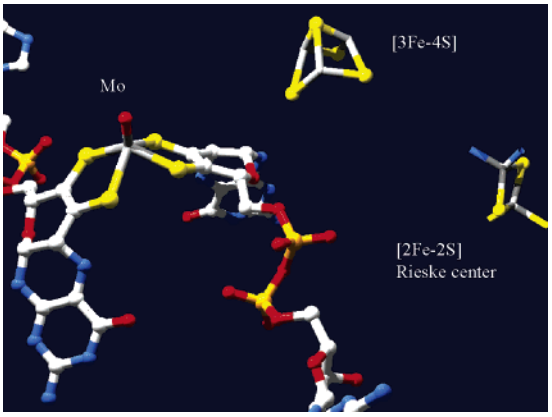

FIGURE 1: Active site of arsenite oxidase from *A. faecalis* (from ref *12*). The Mo active site is in its tetravalent (inactive) oxidation state, and the coordination geometry is square-based pyramidal. In its active hexavalent state, a sixth water-based ligand is present (*11*). The [3Fe-4S] and Rieske-type [2Fe-2S] clusters are also shown.

characteristic of its fully reduced Mo^{IV} form, whereas upon oxidation, a six-coordinate $Mo^{VI}O(X)(MGD)_2$ (X = O or OH) form has been proposed from EXAFS and resonance Raman spectroscopy (*11*). The two Fe−S clusters are arranged in a way that suggests electron egress from the Mo ion after oxidation of arsenite proceeds first via the [3Fe-4S] cluster and then via the Rieske-type [2Fe-2S] cluster before being transferred to its physiological electron partner (azurin or a *c*-type cytochrome). The [3Fe-4S] cluster is approximately equidistant from the Mo and Rieske centers (14−15 Å) (*12*). The overall configuration of NT-26 arsenite oxidase is an $\alpha_2\beta_2$ tetramer, although this is not characteristic of all arsenite oxidases, with $\alpha\beta$ (*13*, *14*) and $\alpha_3\beta_3$ (*15*) stoichiometries known for other enzymes.

In this work, we report the direct electrochemistry of NT-26 arsenite oxidase using the technique of protein film voltammetry (*16*) where the electroactive enzyme is deliberately adsorbed on the working electrode surface while the potential of the electrode is swept both positive and negative of the redox potentials of the cofactors as a function of time. The catalytic current is a direct indicator of enzyme turnover (*17*). Catalysis (in this system) will begin as the applied potential becomes more positive than the redox potentials of the cofactors, where the active site and its electron relays are all in their fully oxidized and active states. Catalysis is sustained by the working electrode in its role as an electron acceptor (in this particular case), thus supplanting the role of the physiological electron transfer partner. A key advantage of direct (unmediated) enzyme electrochemistry is that the potential at which catalysis occurs is linked with redox processes occurring on the enzyme and not masked by the redox potential of an artificial electron transfer mediator. Our electrochemical results are compared with those reported recently for arsenite oxidase from *A. faecalis*.

EXPERIMENTAL PROCEDURES

Reagents. All reagents were analytical grade, and MilliQ water was employed for all experiments.

Enzyme Preparation. The enzyme NT-26 arsenite oxidase was prepared as previously described (*8*) except that the gel filtration buffer 50 mM MES (pH 5.5) also contained 100 mM NaCl. The enzyme was stored at −70 °C as separate 10 μL aliquots each at a concentration of 20 μM.

Electrochemistry. All experiments were conducted with a BAS100B/W potentiostat coupled to a BAS RDE-2 rotating disk electrode cell stand. A platinum wire counter and the Ag/AgCl reference electrode (3 M NaCl, E° = 196 mV vs NHE) were used. All potentials are cited relative to the NHE. A thermostated electrochemical cell was employed, and temperatures in the range of 5−25 °C (±0.1 °C) were set by a Colora Kryo-Thermostat recirculating water bath. No corrections were made for the potential of the reference as a function of temperature. It is known (*18*) that the Ag/AgCl reference electrode exhibits a small temperature variation (~10 mV) between 5 and 25 °C. The cell was purged with nitrogen before the measurement and blanketed with nitrogen during the measurement. The electrochemical cell contained 1 mL of MES buffer (50 mM) and NaCl (10 mM) as the supporting electrolyte. The pH was adjusted by addition of either dilute acetic acid or NaOH. Data analysis was performed with BAS100W version 2.3.

The working electrode was an edge-oriented pyrolytic graphite disk (~0.1 cm^2) that had been cleaned by cleaving several 2 μM layers from its surface with a microtome and then sonicated in water for 1 min. The optimal electrode preparation was obtained using polymyxin sulfate as a co-adsorbate. Specifically, the electrode was dried and inverted while 5 μL of a polymyxin sulfate solution (1%, w/v) was added to the exposed graphite surface. After ca. 10 min, 5 μL of a 20 μM solution of NT-26 arsenite oxidase was added to the somewhat concentrated drop of polymixin sulfate and the electrode was allowed to stand at room temperature for ca. 30 min to allow the enzyme to adsorb on the graphite surface. After this time, the electrode was added to the electrochemical cell comprising a Pt wire counter and the Ag/AgCl reference electrode. A didodecyldimethylammonium bromide (DDAB) surfactant film of the enzyme was also prepared on the electrode surface using published procedures (*19*, *20*).

RESULTS

Enzyme Immobilization. Various enzyme-modified working electrode preparations were explored. The optimal procedure involved using the peptide polymixin sulfate as a (non-redox active) promoter to enhance the surface coverage of the electroactive enzyme. In the absence of polymixin, i.e., adding the enzyme directly to the inverted freshly cleaved pyrolytic graphite electrode, an electroactive enzyme film was still obtained but the catalytic currents were only 20% of those obtained with polymyxin present. Successful experiments were also conducted with an enzyme immobilized within a didodecyldimethylammonium bromide (DDAB) surfactant film. Again the catalytic currents were ~20% of the optimal values. However, in all cases, the same kinetic parameters, relative pH, and temperature dependences were observed (see below) regardless of electrode preparation.

Nonturnover Voltammetry. Despite a number of attempts with different promoters, no convincing cyclic or square wave voltammetric responses could be obtained from NT-26 arsenite oxidase in the absence of substrate. The cyclic voltammogram of NT-26 arsenite oxidase at pH 5.6 and 5

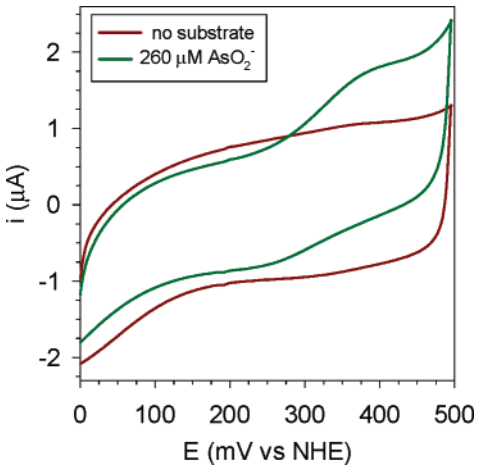

FIGURE 2: Cyclic voltammograms of Aro (co-adsorbed with polymixin) in the absence (red curve) and presence (green curve) of sodium arsenite (260 μM). Experimental conditions: pH 5.6, 5 °C, sweep rate of 5 mV/s, stationary working electrode.

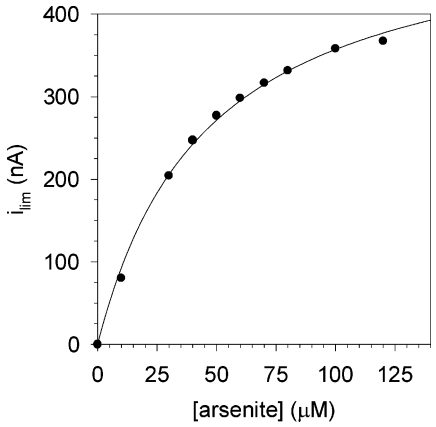

FIGURE 3: Plot of the limiting catalytic current as a function of substrate concentration. The solid curve fit to the Michaelis−Menten equation with a K_M of 46 μM and an i_{max} of 522 nA. Experimental conditions: pH 5.6, 5 °C, sweep rate of 5 mV/s, stationary working electrode, polymixin co-absorbate.

°C in the absence of arsenite is shown in Figure 2 (red curve). The only discernible responses are a pair of broad and weak peaks around 340 mV which are also present in the voltammogram of the clean, untreated pyrolytic graphite electrode and are due to surface redox reactions (quinone/hydroquinone) of the graphite electrode itself (*21*). This response exhibits a pH dependence of −59 mV/pH unit. It is possible that faradaic responses from the enzyme cofactors overlap with this graphite-based signal, but we could not deconvolute these with any confidence. The absence of responses from the Mo active site or the two Fe−S clusters is most probably related to poor surface coverage of the electroactive enzyme. This includes the possibility of a distribution of orientations of the enzyme on the electrode surface, many of which are incapable of undergoing direct heterogeneous electron transfer with the graphite electrode.

Catalytic Voltammetry. In the presence of 260 μM arsenite at pH 5.6 and 5 °C, a sigmoidal voltammetric wave emerges with a half-wave potential of ca. 370 mV versus the NHE (Figure 2, green curve) that is clearly different from that seen in the absence of arsenite (Figure 2, red curve). In a separate experiment, a more gradual addition of arsenite to the electrochemical cell in the presence of the enzyme-modified electrode leads to a steady increase in catalytic current until a plateau is approached around a concentration of 100 μM (Figure 3). The data follow Michaelis−Menten kinetics, and an electrochemical Michaelis constant K_M of 46 μM (pH 5.6) was obtained from the plot shown in Figure 3. Importantly, no arsenite oxidation current was seen in control experiments conducted in the absence of enzyme; i.e., direct (nonspecific) electrochemical oxidation of arsenite is not observed within the potential window shown in Figure 2, and the current is derived from a truly enzymatic process.

$$i_{cat} = nF\Gamma \times \text{turnover number} \quad (1)$$

The electrochemical K_M value (at pH 5.6) determined from experiments with different electrode preparations (polymixin, direct adsorption, DDAB surfactant film) always fell within a relatively narrow range (30 μM < K_M < 50 μM). However, the catalytic current at enzyme saturation and high potential (i_{cat}) varied considerably from one experiment to the next. Equation 1 shows that i_{cat} is directly proportional to the turnover number, the number of electrons in the reaction (n), and the Faraday constant (F). The only variable is the surface coverage of electroactive enzyme (Γ, in moles), and it emerges that this is the parameter that will be responsible for variations in i_{cat} from one experiment to the next (all other things being constant such as temperature and pH). In the absence of nonturnover voltammetric responses, which when integrated enable the surface coverage Γ to be calculated, we are unable to directly quantify the amount of electroactive enzyme on the electrode surface. Solution studies of NT-26 arsenite oxidase at pH 5.5 have found a K_M (arsenite) of 61 μM and a k_{cat} of 4.3 s^{-1} per Mo subunit (*8*). If the enzyme is functioning with the same efficiency on the electrode surface as it would in solution, then eq 1 gives a Γ value of 0.6 pmol, which is lower than a typical monolayer coverage.

Substrate Mass Transport. The catalytic wave in Figure 2 has a somewhat distorted sigmoidal shape with the anodic (forward) sweep appearing more intense than the reverse sweep. Although the wave is superposed on a sloping baseline, thus masking its true form, this feature is indicative of depletion of substrate from the diffusion layer during the anodic sweep as in a normal transient, diffusion-limited cyclic voltammogram.

If the electrode is rotated at 1000 rpm, the wave takes on a truly symmetrical shape and the forward and backward sweeps are identical if the capacitive component of the current is ignored (Figure 4). Voltammograms measured using rotation rates of 500 and 2000 rpm were virtually indistinguishable from that measured at 1000 rpm (Figure S1). The steepness of the catalytic wave is related to the apparent number of electrons (n_{app}) (*17*), also termed the cooperativity coefficient (*22*). This is more easily visualized by taking the first derivative of the voltammogram (Figure S2). The peak width of the derivative at half-height should be approximately $90/n_{app}$ within the temperature range studied here. The peak width seen is around 100 mV which implies a single electron transfer step is rate-limiting. This is most likely one of the two (strictly single electron) Fe−S redox centers (Figure 1) that act as relays of electrons from the Mo active site following arsenite oxidation.

Notwithstanding the subtle differences in waveform going from a stationary to a rotating electrode, the background-

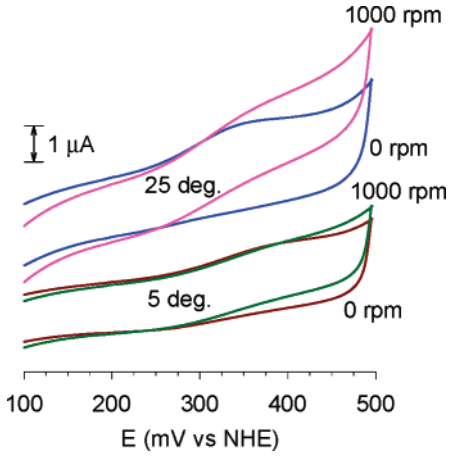

FIGURE 4: Effect of working electrode rotation on cyclic voltammograms of Aro (co-adsorbed with polymixin). Experimental conditions: pH 5.6, 25 °C (top curves) or 5 °C (bottom curves), sweep rate of 5 mV/s. Rotation rates were as indicated.

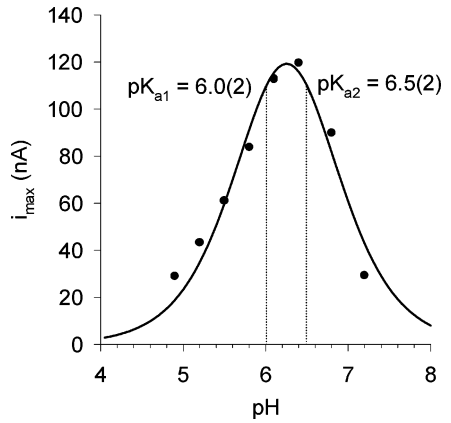

FIGURE 5: pH dependence of the limiting catalytic current of Aro in the presence of 260 μM arsenite. Experimental points fit to a solid curve using eq 2 with pK_a values of 6.0 ± 0.2 and 6.5 ± 0.2. Experimental conditions: 260 μM arsenite, 25 °C, sweep rate of 5 mV/s, stationary working electrode.

subtracted limiting anodic currents are barely distinguishable regardless of the rotation rate (Figure 4). In other words, mass transport of arsenite to the enzyme is not limiting turnover regardless of forced convection through electrode rotation, and turnover is limited by chemical steps associated with the enzyme.

pH Dependence. The saturation catalytic current exhibits a pH optimum of 6.3 and follows a classical "bell-shaped" profile (*23*). The data shown in Figure 5 were modeled well with eq 2 which describes an active form of the enzyme−substrate complex that is deactivated by either protonation [pK_{a1} = 6.0(2)] or deprotonation [pK_{a2} = 6.5(2)].

$$i_{max} = \frac{i_{opt}}{1 + 10^{pK_{a1} - pH} + 10^{pH - pK_{a2}}} \quad (2)$$

The half-wave potential at which catalysis occurs exhibits a pH dependence of −33 mV/pH unit between pH 4.5 and 7 (Figure 6). In the absence of nonturnover signals from the three cofactors, we cannot assign this pH dependence to any particular protonation reaction at this time.

The redox-dependent solution structures of arsenite oxidase from *A. faecalis* have been probed by EXAFS and resonance Raman spectroscopy (*11*). The authors of ref *11* concluded

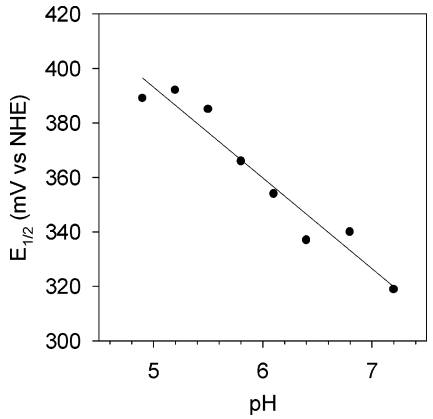

FIGURE 6: Plot of the pH dependence of the catalytic half-wave potential. The solid line is a linear regression of the experimental points and has a slope of −33 mV/pH unit. Experimental conditions were as described in the legend of Figure 4.

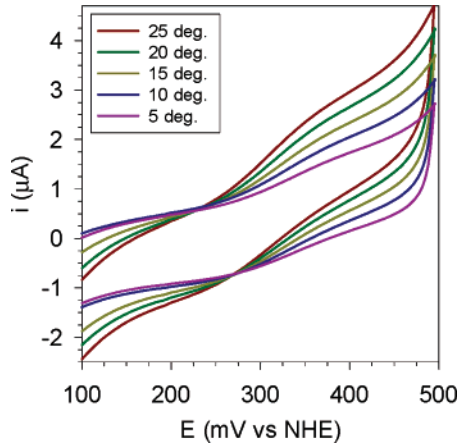

FIGURE 7: Temperature dependence of the catalytic waveform (temperatures as indicated in the legend). Experimental conditions: 260 μM arsenite, pH 5.6, sweep rate of 5 mV/s, working electrode rotation rate of 1000 rpm.

that the structure of the reduced form is most probably the same as that identified crystallographically [$Mo^{IV}O(MGD)_2$]. However, in its oxidized form, two distinct Mo^{VI}−O coordinate bonds were identified as leaving the coordination sphere as either $Mo^{VI}O(OH)(MGD)_2$ or $Mo^{VI}O(O)(MGD)_2$ (with chemically inequivalent oxo ligands).

Temperature Dependence. As expected, the catalytic current is temperature-dependent and increases with temperature from 5 to 25 °C (Figure 7). The five data points enabled construction of an Arrhenius plot (Figure S3), and an approximate activation energy of 27 kJ/mol was obtained for the catalytic reaction. This value is on the order expected for an enzyme-catalyzed reaction (*24*). An additional feature is that the slope of the baseline increases with an increase in temperature, although the precatalytic ($E < E_{cat}$) and postwave (steady state, $E > E_{cat}$) current−voltage curves are essentially parallel.

DISCUSSION

Our electrochemical experiments with NT-26 arsenite oxidase were facilitated by the remarkably robust nature of the enzyme. Enzyme-modified electrodes retained catalytic activity for several days if stored in a refrigerator and immersed in buffer. Catalytic voltammetry could be under-

taken at room temperature with stationary and rotating electrodes without a noticeable loss of activity during the course of the experiment. The pH profile of enzyme activity was established by varying the pH of the solution between pH 4 and 7.5. A pronounced catalytic optimum of pH 6.3 was found, which is slightly higher than that found in solution (pH 5.5) (*7*). Importantly, the pH variations in catalytic current were reversible; i.e., the pH profile was independent of the direction of titration or the order in which data were acquired, and full activity was restored when the solution pH was restored to its optimal value.

There are only a few well-characterized arsenite oxidase enzymes. The one that has been most thoroughly studied is the arsenite oxidase from the soil bacterium *A. faecalis* (*13*, *25*, *26*). The crystal structure of this enzyme has been reported (*12*), and its solution structure has been examined by EXAFS and resonance Raman spectroscopy (*11*). Although phylogenetically NT-26 and *A. faecalis* are unrelated (the latter being a member of the *β-Proteobacteria* while NT-26 is a member of the α-*Proteobacteria*), the α subunits of the arsenite oxidases from both organisms are ∼50% identical (*15*) so their comparative catalytic activities are of interest. In any case, given the similarities between the enzymes, the crystal structure of *A. faecalis* arsenite oxidase (Figure 1) serves as an excellent guide for understanding the properties of NT-26 arsenite oxidase. There has also been a recent report of the direct electrochemistry of *A. faecalis* arsenite oxidase (*22*), and these results are compared with our own.

The three distinct redox centers in arsenite oxidase comprise a single-electron Rieske-type $[2Fe\text{-}2S]^{2+/+}$ couple, a one-electron $[3Fe\text{-}4S]^{+/0}$ couple, and the Mo active site which may reside in the Mo^{VI}, Mo^{V}, or Mo^{IV} state. Resolution of separate $Mo^{VI/V}$ and $Mo^{V/IV}$ couples depends on the relative redox potentials of these couples. If $E°(Mo^{VI/V}) < E°(Mo^{V/IV})$, then a cooperative two-electron transfer may occur; i.e., the EPR active Mo^{V} form is never observed. Indeed, there is evidence to suggest that this is the case in the arsenite oxidase from *A. faecalis* where no EPR signal could be elicited from the Mo center during a titration with arsenite (*13*). More recent electrochemical work with the enzyme reported (*22*) a two-electron voltammetric response from the Mo center (at 292 mV vs the NHE at pH 6.0). No voltammetric responses from the two Fe−S clusters were found, and their potentials were determined by a mediated optical redox potentiometry titration. This analysis was complicated by the fact that arsenite oxidase exhibits very weak optical absorbance change in the visible region upon reduction and is thus a less than ideal system for investigation by this method, unlike stronger chromophores such as heme and flavin-dependent proteins. The redox potentials of the two Fe−S clusters of *A. faecalis* arsenite oxidase were reported to be 130 mV ($[2Fe\text{-}2S]^{2+/+}$) and 260−270 mV ($[3Fe\text{-}4S]^{+/0}$) (vs the NHE at pH 6.0) (*22*).

There are some notable comparisons and contrasts that can be made between the electrochemical behavior of NT-26 and *A. faecalis* arsenite oxidase (*22*). First, the potentials at which catalysis occurs are similar at pH 6.0. However, the pH dependence of the catalytic wave potentials for NT-26 arsenite oxidase appears to follow the predicted trend for a two-electron, single-proton process (slope of −29.6 mV/pH unit at 298 K). Limited pH-dependent data were reported (pH 6.0, 7.0, and 7.9) for the catalytic potential of *A. faecalis* arsenite oxidase (*22*). The actual catalytic half-wave potentials from that study may only be estimated from a figure, but the authors indicated that the pH dependence of the catalytic wave was similar to that of the nonturnover response from the Mo active site, i.e., a two-electron, two-proton reaction. It appears that an interesting difference has emerged here between the catalytic mechanisms of these two enzymes from disparate organisms.

The relatively straightforward catalytic voltammetric behavior of NT-26 arsenite oxidase contrasts with the complicated waveforms reported for *A. faecalis* arsenite oxidase (*22*). The authors reported significant departures from the expected sigmoidal voltammetric waveform as either the temperature or the substrate concentration was increased. Specifically, at either saturating concentrations of substrate or temperatures above ∼20 °C, the maximum catalytic current (at high potential) did not reach a plateau (even after correction for background current). This is problematic as it masked both the limiting catalytic current and the half-wave potential at which catalysis occurs.

As mentioned, we saw no temperature- or substrate-dependent phenomena associated with the shape of the catalytic voltammetric wave. Instead, the catalytic currents exhibited variations in accord with a simple Arrhenius behavior (Figure S3) and Michaelis−Menten kinetics (substrate). Regardless of the temperature or substrate concentration, the pre- and postwave regions of the voltammogram were essentially parallel and the limiting (background subtracted) currents and catalytic potentials could be determined directly from the raw data using the instrument software. We did see an increase in the slope of the overall uncorrected voltammogram as a function of temperature (Figure 7), but this change is probably related to nonfaradic temperature effects relating to the graphite electrode rather than any intrinsic temperature-dependent catalytic properties of the enzyme.

The redox potentials of the cofactors in NT-26 arsenite oxidase remain unknown at present, and their determination will require other techniques such as EPR spectroscopy (for the Fe−S cluster on the assumption that the Mo cofactor will not give a Mo^{V} EPR signal) or optical potentiometry at protein concentrations higher than those that are at present practical given the amount of enzyme at our disposal. A high-yield expression system for NT-26 arsenite oxidase may enable these experiments to be carried out soon.

The absence of nonturnover signals in our voltammetric experiments with NT-26 arsenite oxidase precludes a direct measure of the surface concentration of the adsorbed and electroactive enzyme. On the assumption that the enzyme is capable of turning over arsenite at a rate similar to its rate in solution, we have a submonolayer coverage of the enzyme on the electrode. This was achieved with polymixin as a co-adsorbate, and other methods of protein adsorption led to less than 20% of this activity. Other methods of enzyme confinement may prove to be more efficient than those reported here, particularly in eliciting nonturnover responses from the enzyme, but at present, we have established that the enzyme is robust and active on the working electrode and serves as an ideal system for studying by direct protein film voltammetry.

CONCLUSIONS

Stable and reproducible catalytic voltammetry of NT-26 arsenite oxidase has been reported at an applied electrochemical potential in the range 300−400 mV versus the NHE. The substrate concentration dependence of the catalytic current follows Michaelis−Menten kinetics, and an electrochemical K_M value similar to that reported for the enzyme in solution was identified. The catalytic current also exhibited a temperature dependence consistent with a typical enzyme-catalyzed reaction.

SUPPORTING INFORMATION AVAILABLE

Cyclic voltammograms at rotation rates of 500, 1000, and 2000 rpm and an Arrhenius plot of the temperature dependence of the catalytic current. This material is available free of charge via the Internet at http://pubs.acs.org.

REFERENCES

1. Thomas, D. J., Styblo, M., and Lin, S. (2001) The Cellular Metabolism and Systemic Toxicity of Arsenic, *Toxicol. Appl. Pharmacol. 176*, 127−144.
2. Hughes, M. F. (2002) Arsenic toxicity and potential mechanisms of action, *Toxicol. Lett. 133*, 1−16.
3. Mandal, B. K., and Suzuki, K. T. (2002) Arsenic round the world: A review, *Talanta 58*, 201−235.
4. Tchounwou, P. B., Patlolla, A. K., and Centeno, J. A. (2003) Carcinogenic and Systemic Health Effects Associated with Arsenic Exposure: A Critical Review, *Toxicol. Pathol. 31*, 575−588.
5. Eisler, R. (2004) Arsenic hazards to humans, plants, and animals from gold mining, *Rev. Environ. Contam. Toxicol. 180*, 133−165.
6. Brown, K. G., and Ross, G. L. (2002) Arsenic, Drinking Water, and Health: A Position Paper of the American Council on Science and Health, *Regul. Toxicol. Pharmacol. 36*, 162−174.
7. Santini, J. M., Sly, L. I., Schnagl, R. D., and Macy, J. M. (2000) A new chemolithoautotrophic arsenite-oxidizing bacterium isolated from a gold mine: Phylogenetic, physiological, and preliminary biochemical studies, *Appl. Environ. Microbiol. 66*, 92−97.
8. Santini, J. M., and vanden Hoven, R. N. (2004) Molybdenum-containing arsenite oxidase of the chemolithoautotrophic arsenite oxidizer NT-26, *J. Bacteriol. 186*, 1614−1619.
9. Lebrun, E., Brugna, M., Baymann, F., Muller, D., Lievremont, D., Lett, M.-C., and Nitschke, W. (2003) Arsenite oxidase, an ancient bioenergetic enzyme, *Mol. Biol. Evol. 20*, 686−693.
10. Hille, R. (1996) The mononuclear molybdenum enzymes, *Chem. Rev. 96*, 2757−2816.
11. Conrads, T., Hemann, C., George, G. N., Pickering, I. J., Prince, R. C., and Hille, R. (2002) The Active Site of Arsenite Oxidase from *Alcaligenes faecalis*, *J. Am. Chem. Soc. 124*, 11276−11277.
12. Ellis, P. J., Conrads, T., Hille, R., and Kuhn, P. (2001) Crystal structure of the 100 kDa arsenite oxidase from *Alcaligenes faecalis* in two crystal forms at 1.64 Å and 2.03 Å, *Structure 9*, 125−132.
13. Anderson, G. L., Williams, J., and Hille, R. (1992) The purification and characterization of arsenite oxidase from *Alcaligenes faecalis*, a molybdenum-containing hydroxylase, *J. Biol. Chem. 267*, 23674−23682.
14. Muller, D., Lievremont, D., Simeonova, D. D., Hubert, J.-C., and Lett, M.-C. (2003) Arsenite oxidase aox genes from a metal-resistant β-proteobacterium, *J. Bacteriol. 185*, 135−141.
15. vanden Hoven, R. N., and Santini, J. M. (2004) Arsenite oxidation by the heterotroph *Hydrogenophaga* sp. str. NT-14: The arsenite oxidase and its physiological electron acceptor, *Biochim. Biophys. Acta 1656*, 148−155.
16. Armstrong, F. A., and Wilson, G. S. (2000) Recent developments in faradaic bioelectrochemistry, *Electrochim. Acta 45*, 2623−2645.
17. Heering, H. A., Hirst, J., and Armstrong, F. A. (1998) Interpreting the Catalytic Voltammetry of Electroactive Enzymes Adsorbed on Electrodes, *J. Phys. Chem. B 102*, 6889−6902.
18. Ives, D. J. G., and Janz, G. J. (1961) *Reference Electrodes. Theory and Practice*, Academic Press, New York.
19. Rusling, J. F. (1998) Enzyme Bioelectrochemistry in Cast Biomembrane-Like Films, *Acc. Chem. Res. 31*, 363−369.
20. Aguey-Zinsou, K.-F., Bernhardt, P. V., Kappler, U., and McEwan, A. G. (2003) Direct Electrochemistry of a Bacterial Sulfite Dehydrogenase, *J. Am. Chem. Soc. 125*, 530−535.
21. Evans, J. F., and Kuwana, T. (1977) Radiofrequency oxygen plasma treatment of pyrolytic graphite electrode surfaces, *Anal. Chem. 49*, 1632−1635.
22. Hoke, K. R., Cobb, N., Armstrong, F. A., and Hille, R. (2004) Electrochemical Studies of Arsenite Oxidase: An Unusual Example of a Highly Cooperative Two-Electron Molybdenum Center, *Biochemistry 43*, 1667−1674.
23. Brody, M. S., and Hille, R. (1999) The Kinetic Behavior of Chicken Liver Sulfite Oxidase, *Biochemistry 38*, 6668−6677.
24. Wolfenden, R., Snider, M., Ridgway, C., and Miller, B. (1999) The Temperature Dependence of Enzyme Rate Enhancements, *J. Am. Chem. Soc. 121*, 7419−7420.
25. McNellis, L., and Anderson, G. L. (1998) Redox-state dependent chemical inactivation of arsenite oxidase, *J. Inorg. Biochem. 69*, 253−257.
26. Anderson, G. L., Ellis, P. J., Kuhn, P., and Hille, R. (2002) Oxidation of arsenite by *Alcaligenes faecalis*, *Environ. Chem. Arsenic*, 343−361.

BI0522448